Geosci. Model Dev. Discuss., 8, 2807–2845, 2015
www.geosci-model-dev-discuss.net/8/2807/2015/
doi:10.5194/gmdd-8-2807-2015

Geoscientific Model Development Discussions
Open Access

Assessment of the uncertainty of snowpack simulations based on variance decomposition

T. Sauter[1,2] and F. Obleitner[1]

[1]Institute of Meteorology and Geophysics, University of Innsbruck, Innsbruck, Austria
[2]Institute of Geography, University of Erlangen-Nuremberg, Erlangen, Germany

Received: 8 January 2015 – Accepted: 13 February 2015 – Published: 13 March 2015

Correspondence to: T. Sauter (tobias.sauter@uibk.ac.at)

Published by Copernicus Publications on behalf of the European Geosciences Union.

Abstract

State of the art numerical snow models essentially rely on observational data for initialization, forcing, parametrization and validation. Such data are available in increasing amount, but the inherent propagation of related uncertainties on the simulation results has received rather limited attention so far. Depending on their complexity, even small errors can have a profound effect on simulations, which dilutes our confidence in the results. This paper quantifies the fractional contributions of some archetypical measurement uncertainties on key simulation results in a high Arctic environment. The contribution of individual factors on the model variance, either alone or by interaction, is decomposed using *Global Sensitivity Analysis*. The work focuses on the temporal evolution of the fractional contribution of different sources on the model uncertainty, which provides a more detailed understanding of the model's sensitivity pattern. The decompositions demonstrate, that the impact of measurement errors on calculated snow depth and the surface energy balance components varies significantly throughout the year. Some factors show episodically strong impacts, although there overall mean contribution is low while others constantly affect the results. However, these results are not yet to be generalized imposing the need to further investigate the issue for e.g. other glaciological and meteorological settings.

1 Introduction

Snow is a key component of the earth system, which has a vital importance for the structure and dynamics of the atmospheric boundary layer by modifying e.g. the exchange processes between the atmosphere and the underlying ground. Bridging the gap between the inherent microphysical snow processes and the exchange processes at the snow surface still constitutes major challenges to scientists. With this in mind, snow scientists have done much research during the last years improving our knowledge and understanding of the associated processes. Our theoretical understanding is

GMDD

8, 2807–2845, 2015

largely derived from observations, which provide the basis for numerical models which frequently have to employ parametrizations of processes which yet cannot explicitly be treated at the model grid or in terms of the prognostic variables. Sophisticated snow models summarize our present knowledge and prove themselves to be a useful tool in simulating the spatial and temporal evolution of snowpacks. As reported in many studies, snow models have been successfully applied and implemented for climate impact studies (e.g. Durand et al., 2009), avalanche forecasting (e.g. Bellaire et al., 2013; Durand et al., 1999; Lehning et al., 1999), glacier modelling (e.g. Obleitner and Lehning, 2004; Gallée et al., 2001) and hydrological research (e.g. Magnusson et al., 2014; Lehning et al., 2006; Liston and Elder, 2006; Bernhardt et al., 2010). Snow models currently used can be roughly classified by their degree of complexity, ranging from simplified single-layer models through to detailed physical snowpack models (Etchevers et al., 2004; Feng et al., 2008; Rutter et al., 2009). Besides all advantages of detailed models, the increasing complexity leads inevitably to higher demands on the kind and quality of data required to force these models. However, the "true" value of a measured quantity is rather a theoretical concept, and can often not be determined. In view of this uncertainty, we usually estimate a range of values within which the true value is likely to fall. Ideally, these uncertainties should be considered in the modelling process and when interpreting results – not at least to ensure good scientific practise. However, in practise it is not always easy to derive a reliable probability density function describing the inherent uncertainty of input data and model parameters (see Sect. 3.2). Taking into account systematic measurement errors allow scientists quantifying the uncertainty in the model outcome, and providing information on its robustness. A kind of minimum approach is through Monte Carlo analysis by randomly drawing samples for each input factor from previously derived distribution functions. From the model we can compute first and higher moment statistics to quantify the integrated model uncertainty. In this context, integrated is understood as the total effect of all measurement or parameter uncertainties on the model's variability. At this point, there is still no information on how uncertainty in the model output can be apportioned to different sources of uncertainty

GMDD
8, 2807–2845, 2015

in the input data set or parameter setting. Since with increasing degree of model complexity sub-routines or modules become highly coupled, unambiguous allocation of the uncertainty of model parameters and forcing data on the model's variance is hampered by interaction effects. To achieve a full understanding of the model's sensitivity pattern, in particular of highly interconnected and nonlinear models such as sophisticated snow models, it is necessary to decompose the complete variance of the model results.

In recent years there have been an increasing awareness of the issue yielding efforts to quantify the uncertainty associated with the various sources of error in the parameter setting to assess parametric and predictive uncertainty (e.g. Franz et al., 2010; He et al., 2011; Schmucki et al., 2014; Gurgiser et al., 2013). Efforts to assess the climate sensitivity of snow and glaciers based on mass and energy balance models go into the same direction (e.g. Gerbaux et al., 2005; Fujita, 2008; Radić and Hock, 2006; Greuell and Oerlemans, 1986; Oerlemans, 1992; Braithwaite and Zhang, 2000). However, thorough investigation of the specific influence of uncertainties related to model input and its effect on energy and mass balance calculations received rather scant attention (e.g. Karner et al., 2013; Van de Wal and Oerlemans, 1994; Greuell and Konzelmann, 1994).

The present study intends to contribute to our understanding on how systematic measurement errors and uncertainties of some critical factors influence our confidence in snowpack simulations. We study this effects using the snowpack model CROCUS, which is applied at a study site on the Kongsvegen Glacier in Svalbard (see Sect. 2.2). CROCUS has been developed and is used for operational snow avalanche warning (Brun et al., 1992; Durand et al., 2009), and has been applied to various research problems, e.g. Brun et al. (2013); Fréville et al. (2014); Carmagnola et al. (2013); Wang et al. (2013); Phan et al. (2014); Gallet et al. (2014); Castebrunet et al. (2014). Vionnet et al. (2012) give a comprehensive review of CROCUS and its implementation in SURFEX, i.e. a model platform for simulation of earth surface processes. The results of our study may not yet be generalized due to the rather local nature of our simulations, but it may be useful for other studies using sophisticated snow models in similar environmental settings. A better understanding of the model's sensitivity can be very

GMDD
8, 2807–2845, 2015

helpful to establish priorities in research, identify critical regions in the input space and even for policy assessment. An attractive approach to estimate sensitivity measures independently of the degree of linearity (model-free) is based on the Global Sensitivity Analysis (GSA), which is introduced in Sect. 2.3. Before finally dealing with the decomposition of the model uncertainty in Sect. 3.3, we first perform a common Monte-Carlo uncertainty estimation on a validated reference run (see Sects. 3.1 and 3.2). In the last section we discuss the information gained from the analysis, limitations of linear sensitivity measures, general problems of sensitivity analysis and what can be learned from this analysis.

2 Data and methods

2.1 CROCUS model setup

CROCUS is a physical, finite-element and one-dimensional multilayer snow scheme implemented in the land-surface model ISBA of the surface modelling platform SURFEX. Snow is considered as a porous material whose properties are determined by the microstructure characteristics – grain size, dendricity, and sphericity. These properties mainly describe porosity, diffusivity, heat conductivity, viscosity, or extinction of radiation. The evolution of the microstructure characteristics is closely linked to the prevailing environmental conditions and the related exchange processes. Snow metamorphism laws for the evolution of types and size of the snow grains have been derived from empirical observations and are implemented by parametrizations.

The model is extensively described elsewhere (Vionnet et al., 2012; Brun et al., 1992) and we therefore give just a basic description and note modifications important for this study. CROCUS is a one-dimensional snow model which simulates the evolution of the physical and morphological snow properties depending on the atmospheric and basal boundary conditions. It thereby considers the conservation of energy and mass within layered control volumes and the associated processes (molecular conduc-

Discussion Paper | Discussion Paper | Discussion Paper | Discussion Paper |

GMDD

8, 2807–2845, 2015

Assessment of the uncertainty of snowpack simulations

T. Sauter and F. Obleitner

tion, radiative transfer, turbulent exchange of sensible and latent heat, phase changes and gravitational water transport). Snow layers are described through bulk physical properties (thickness, density, temperature, liquid water content) and microstructure parameters (dendricity, sphericity, grain size and indicators of the of snow grain history). The latter enables CROCUS to describe the changes in the morphological shape of snow crystals depending on snow metamorphism in response to atmospheric forcing and internal processes. To adequately treat these processes, the model employs a number of parametrizations derived from specific field and laboratory experiments. The governing equations are numerically solved in a vertical domain with space and time varying grid distances (necessary in order to cope with e.g. settling processes). The model is forced by the basic meteorological parameters (air temperature, humidity, wind speed and precipitation rate as well as incoming solar and infrared radiation) and is initialized by vertical profiles of key physical properties of snow and its underlying substrate. Model output comprises the vertical profiles of the bulk physical (snow temperature, density, liquid water content) and structure parameters as well as prognostic time series of surface temperature, snow depth and energy- and mass balance components, the latter two being coupled. Following e.g. Armstrong and Brun (2008), the change of internal energy

$$-\frac{\mathrm{d}E}{\mathrm{d}t} = \mathrm{NR} + \mathrm{SHF} + \mathrm{LHF} + R + G \tag{1}$$

$$= L_{\mathrm{li}}(R_{\mathrm{f}} - R_{\mathrm{M}}) - \int_{z=0}^{\mathrm{HS}} \left[\frac{\mathrm{d}}{\mathrm{d}t}(\rho_z c_p T_z)\right] \mathrm{d}z, \tag{2}$$

of the snowpack depends on the surface energy budget (SEB), i.e. the sum of net radiation NR, the turbulent fluxes of sensible (SHF) and latent heat (LHF), the heat transfered by precipitation and blowing snow (R), and by conduction from the underlying material G (glacier ice in our case). Thus available energy can be used for changes in cold content of the snow pack throughout its total depth HS (right-hand term in

GMDD
8, 2807–2845, 2015

Eq. 2) or phase changes (melt or freeze; first-hand term in Eq. 2). R_f and R_M are the freezing and melting rate, L_li the latent heat of fusion of ice ($3.34 \times 10^5\,\mathrm{J\,kg^{-1}}$), c_p the specific heat capacity of ice ($2.1 \times 10^3\,\mathrm{J\,kg^{-1}\,K^{-1}}$), ρ_z and T_z denote the density and snow temperature at depth z. Net radiation itself is composed of the sum of incoming and outgoing solar- and infrared radiation (measured input except of outgoing infrared) and the turbulent fluxes are parametrized following the standard micrometeorological framework based on Monin–Obukhov similarity theory.

The according changes in available energy induce either varying cold content (warming/cooling; last term of Eq. 2) or phase changes of individual snow layers (Eq. 3, right hand terms). Melt water refreezing and/or sublimation rates (E) as well as runoff (R_runoff) couple the energy- and the mass budget of a snow pack according to

$$\frac{\mathrm{d}M}{\mathrm{d}t} = P \pm E - R_\mathrm{runoff}. \tag{3}$$

Key parameters of this coupled system will be addressed in this study, too. CROCUS has not yet been applied to Kongsvegen before. The following paragraphs summarize the main modifications and setup used in this study.

Water flow and refreezing. Superimposed ice is a common feature of Arctic glaciers, and a better understanding of the relevant processes is currently an active field of research. We refer as superimposed ice all water which percolates through the snowpack and refreezes on the glacier surface (Wright et al., 2007; Brandt et al., 2008; König et al., 2002). Obleitner and Lehning (2004) and Karner et al. (2013) showed, that on Kongsvegen glacier the superimposed ice layer can reach a thickness of several decimetres in some years. The water percolation and refreezing routine in the current CROCUS version basically simulates the gravitational water flow through the snowpack. The energy available for refreezing is calculated at the beginning of each iteration step. If the snow layer temperature is below the melting point water refreezes and the residual liquid water is retained up to a maximum holding capacity. The maximum liquid water holding capacity PVOL is usually assumed to be 5 % of the total pore

GMDD
8, 2807–2845, 2015

volume. The refreezing process increases the average density and mass of concerned layers (Vionnet et al., 2012). This implementation does not account for superimposed ice, since the water percolates through the glacier ice. To overcome the issue, all water exceeding the maximum liquid water holding capacity at an impermeable snow–ice interface is assumed to contribute to the runoff, and the water flow to next layer is simply set to zero. This modification avoids, that the scheme removes too much water to deeper layers, which limits the refreezing potential (Obleitner and Lehning, 2004).

Model input/output. The CROCUS model is forced by air temperature, specific humidity, wind speed, incoming radiation, precipitation rate and atmospheric pressure (see Sect. 2.2). These time-dependent factors are provided by Netcdf-file. Besides the time-dependent forcing file, a constant model parameters are provided by a static option file. In order to perform Monte-Carlo simulations we have included the roughness length for fresh snow as well as the fraction of total pore volume in the Netcdf-file, used to calculate the maximum holding capacity in the forcing file.

2.2 Input data

To run the snowpack scheme CROCUS we use meteorological and glaciological observations on the Kongsvegen Glacier (78.75° N, 13.33° E, 668 m a.s.l.), located in north-eastern Svalbard. The Kongsvegen currently covers a total surface area of $\sim 100\,\mathrm{km}^2$ and extends over a total length of 26 km. From the highest point (750 m a.s.l.) in the east, the glacier flows north-eastwards towards the north west coast. Several automatic weather stations are operated along the flow line of the glacier, of which this study only makes use of the station KNG8 operated in the accumulation zone (see Fig. 1). Due to computational limitations we had to restrict our error analysis to a one-year period.

The station is equipped with state of the art sensors for air temperature, relative humidity, wind speed, and direction as well as the shortwave and longwave radiation components. Surface height changes were measured by an ultrasonic ranger. Karner et al. (2013) performed a comprehensive data quality assessment and correction of unreliable observations. The processed data are available as hourly averages and enhanced quality checking of the data suggested to apply some further corrections:

Filling remaining data gaps. For shorter gaps the missing values have been estimated by linear regression from surrounding stations, where it was possible. In cases this was not possible, e.g. because the surrounding stations showed also gaps, the missing values have been estimated by a stochastic nearest-neighbour resampling conditioned on the remaining variables (Beersma and Buishand, 2003). This was achieved by first calculating the euclidean distance between the present day and all other days without gaps. Based to the distance one out of the 20 closest days have been stochastically selected and the missing value has been replaced by the corresponding value. This approach is convenient for small gaps and guarantees physical consistent fields.

Conversion of snow depth changes to water equivalent. Snow precipitation rates were derived from surface height changes measured by the ultrasonic ranger, and needed to be converted to snow water equivalent (SWE) for input to the model. The density of freshly fallen snow ρ_{new} was calculated according to the equation used by CROCUS, which is a function of wind speed U, and air temperature T_{air}, given as

$$\rho_{new} = a_\rho + b_\rho \cdot (T_{air} - 273.16) + c_\rho \cdot \sqrt{U}, \tag{4}$$

where $a_\rho = 300\,\mathrm{kg\,m^{-3}}$, $b_\rho = 6\,\mathrm{kg\,m^{-3}\,K^{-1}}$, and $c_\rho = 26\,\mathrm{kg\,m^{-7/2}\,s^{-1/2}}$. Note, that in the original model version a_ρ is set to $109\,\mathrm{kg\,m^{-3}}$. We modified this value since the CROCUS model underestimated the initial settling and compaction of the upper snow layers, and has revealed best results concerning the simulated density profile. According to point snow-cover data from snow-pit studies, the mean density of the snowpack in the upper few centimetres usually lies in the range of 100–200 $\mathrm{kg\,m^{-3}}$. It was further necessary to reduce the amount of noise in the original snow records in order to avoid erratic precipitation events, which lead to unrealistic high accumulation. The main factors that affect the sensor signal are blowing snow, intense snowfall, uneven snow surfaces, extreme temperatures and snow crystal type (low density). Blowing and drifting snow are frequent processes in the European Arctic and often result in the formation of sastrugi (Sauter et al., 2013). The associated small scale variability is usually reduced by moving average filter, but the very different event durations make it sometimes difficult to determine an appropriate fixed subset size. We decided to take the mean saltation trajectory height as a measure of the uncertainty, which is assumed to be proportional to the surface shear stress u_*^2 [$\mathrm{m^2\,s^{-2}}$] (Pomeroy and Gray, 1990),

$$h_{\mathrm{salt}} = \frac{1.6 \cdot u_*^2}{2 \cdot g}, \tag{5}$$

where g [$\mathrm{m\,s^{-2}}$] is the gravitational acceleration. The surface shear stress has been estimated from the logarithmic wind profile and an arbitrary chosen constant roughness length of $z_0 = 0.02\,\mathrm{m}$. Finally, snow depth smaller than $0.8 \cdot h_{\mathrm{salt}}$ were considered as noise. The factors z_0 and 0.8 are used for calibration and determine how much signal were removed from the original time series. Filtering out the small scale variability reduced the total precipitation amount at KNG8 by 29 %, and yields a simulated end-winter snow accumulation which is well validated by independent stake observations.

Large amplitude spikes. Large amplitude data spikes in recorded snow depth changes can occur during intense snowfall events when snow particles obstructs the propagation of the senor signal (ultra-sonic pulses). Sudden snow depth changes greater than $50\,\mathrm{mm\,h^{-1}}$ are assumed to belong to this class of events, and were simply ignored. Transition from rain to snow was assumed to take place in the range from 0 to 1 °C with half of the precipitation falling as snow, and the other half as rain. There was no direct information available to determine this threshold better, which leaves a relative large uncertainty.

2.3 Global Sensitivity Analysis (GSA)

In general, sensitivity analysis (SA) permits inferences on the different sources of uncertainty in model inputs by decomposing the variance of the model output

GMDD
8, 2807–2845, 2015

(Sauter and Venema, 2011). This section gives an overview how model-free sensitivity measures can be derived from variance-based methods. For the purpose of illustration lets assume a generic model f

$$\mathbf{Y} = f(\mathbf{X}_1, \mathbf{X}_2, \cdots, \mathbf{X}_k), \tag{6}$$

with the model output $\mathbf{Y}$, the input quantity $\mathbf{X}_k$, and the corresponding total or unconditional variance $V(\mathbf{Y})$. Most common SA measures are based on local derivatives $\partial\mathbf{Y}/\partial\mathbf{X}_k$ to estimate the relative importance of individual quantities. It is convenient to normalize the derivatives by the SD, so that the measures are weighted and sum up to one. In this context it is also interesting to note, that in case of linear models the normalized derivatives coincide with the well known standardized (linear) regression coefficients (Saltelli et al., 2006). Obviously, both measures rely on the assumption of linearity which makes them unsuitable for complex models. This is in particular true when interaction effects become important, a characteristic property of nonlinear and non-additive models. Such effects are captured by so-called model-free measures, which can be effectively estimated by the Global Sensitivity Analysis (GSA) method described here.

If one forcing input $\mathbf{X}_i$ is fixed at a particular value x_i^*, the resulting conditional variance of $\mathbf{Y}$ is accordingly $V_{X\sim i}(\mathbf{Y}|\mathbf{X}_i = x_i^*)$. This measure characterizes the relative importance of the factor $\mathbf{X}_i$, since the conditional variance will be less than the unconditional variance. The fact that, this sensitivity measure depends on the value of x_i^* makes it rather impractical. Taking instead the average of this measure over the uncertainty distribution of x_i^*, the undesired dependence will disappear (Saltelli et al., 1999, 2006). We can obtain following expression

$$V(\mathbf{Y}) = E_{X_i}(V_{X\sim i}(\mathbf{Y}|\mathbf{X}_i = x_i^*)) + V_{X_i}(E_{X\sim i}(\mathbf{Y}|\mathbf{X}_i = x_i^*)), \tag{7}$$

GMDD
8, 2807–2845, 2015

Assessment of the uncertainty of snowpack simulations

T. Sauter and F. Obleitner

where the second conditional variance on the right hand side is called the first-order effect of $\mathbf{X}_i$ on $\mathbf{Y}$. The corresponding first-order sensitivity index of $\mathbf{X}_i$ is given by

$$S_i = \frac{V_{X_i}(E_{X\sim i}(\mathbf{Y}|\mathbf{X}_i = x_i^*))}{V(\mathbf{Y})}. \tag{8}$$

This sensitivity index indicates the importance of individual factors without considering interactions effects. In case the model belongs to the class of additive models, the first-order terms add up to one, e.g. $\sum_{i=1}^{r} S_i = 1$. If this is not the case, the remaining variance must be explained by the higher-order effects (interaction) between input factor uncertainties. Interactions represent an important feature, especially, of nonlinear non-additive models. The total sensitivity S_{T_i} of a factor $\mathbf{X}_i$ is made up of the first- and all higher order terms where a given factor $\mathbf{X}_i$ is participating, consequently giving information on the non-additive character of the model. The S_{T_i} can be computed using,

$$S_{\mathrm{T}_i} = \frac{E(V(\mathbf{Y}|\mathbf{X}_{\sim i}))}{V(\mathbf{Y})}, \tag{9}$$

where $\mathbf{X}_{\sim i}$ indicates that all factors have been fixed and only $\mathbf{X}_i$ varies over its uncertainty range. This approach permits, even for non-additive models, to recover the complete variance of $\mathbf{Y}$. The sum of S_{T_i} is equal to one for perfectly additive models otherwise it is always greater than one. The difference between S_i and S_{T_i} is a useful measure of how much each factor is involved in interactions with any other factor (Saltelli et al., 2010). The indices can be efficiently computed by Monte-Carlo based numerical procedures (Saltelli et al., 2010; Sobol et al., 2007).

GMDD
8, 2807–2845, 2015

3 Results

3.1 Reference run

The reference run serves as basis for the uncertainty estimation of the simulation results (see Sect. 3.2), and the corresponding decomposition of the model variance (see Sect. 3.3). The modified CROCUS model (see Sect. 2.1) is forced with the pre-processed and corrected input data introduced in Sect. 2.2. Most relevant model parameters are given in Table 1. The initial snowpack is assumed to be isotherm with 273.16 K, and a constant base temperature of 271 K. The maximum number of snow layers is set to 50 in order to get a detailed snowpack stratigraphy. The initial grid spacing increases from 0.01 m at the surface to 10 m at the bottom. The number of grid cells and their spacing is updated during the simulation according to the accumulation, temperature, density and melt. The KNG8 is located in the accumulation zone of the glacier where the near surface layers consist of perennial snow rather than bare ice (Björnsson et al., 1996; Brandt et al., 2008). Following Björnsson et al. (1996) and Brandt et al. (2008), the model is initialized with an isothermal firn layer with a mean density of 600 kg m^{-3} and a total thickness of 20.51 m. The starting date is chosen to be the end of the ablation season, with the lowest recorded snow depth. Based on this initialisation set up, the one-year simulation period starts at 11 August 2010 and ends at 10 August 2011. The model is forced by hourly data, whereas results are saved every 6 h for analysis. Measurements of surface temperature, shortwave radiation, albedo, and a snow pit profile in spring are available for validation. Note, that these data have not been used as model input. Comparison of the simulation with the snow pit profile from 6 April 2010 shows a difference in snow depth at the end of the winter period of less than 0.1 m. The simulated mass gain amounts +0.76 mm water equivalent, which corresponds approximately with the observed mass gain of +0.82 mm. Figure 2 shows the comparison of simulated snow surface temperature with observational data computed from upwelling longwave radiation. Surface temperature is a key variable for flux parametrizations. The temporal variability is well captured (R^2 = 0.93), and 95 % of the

GMDD
8, 2807–2845, 2015

absolute deviations are within ±1.1 K and conforms to the general skill of most sophisticated snow models (Obleitner and De Wolde, 1999; Rutter et al., 2009; Etchevers et al., 2004). The spread increases in the winter time, which might in part be associated to undetected riming of the sensor or diverse model uncertainties. The vertical temperature gradient is an important driver of snow metamorphism and is depicted in Fig. 3. In the upper 0.6 m the observed temperature is slightly higher than modelled and the RMSE=1 K is in part attributed to measurements shortcomings as well (Obleitner and De Wolde, 1999). The corresponding density profile confirm that the model is able to simulate the gross snowpack layering (see Fig. 5). The relatively large difference within the upper 0.1 m is due to the fact, that the constant a_ρ in Eq. (4) is set to 300 $\mathrm{kg\,m^{-3}}$. Although this leads to rather high fresh snow densities, the choice is justified when comparing the daily mean snow albedo (see Fig. 4). Albedo here denotes broad-band reflectivity of the snow surface, which is a key parameter determining net radiation. The RMSE of the albedo over the entire simulation period is 0.06 [–]. Albedo ranges between 0.65 in the ablation period and 0.92 in the accumulation period.

Following we indicate some gross features of the seasonal evolution of the energy balance components. The annual longwave radiation budget is negative on average (−18.7 $\mathrm{W\,m^2}$), with enhanced losses during early summer. The yearly average of net radiation is slightly negative (−1.7 $\mathrm{W\,m^2}$). An enhanced energy deficit (−13.2 $\mathrm{W\,m^2}$) is observed during the accumulation period when the incoming shortwave radiation is zero due to polar-night conditions. The energy deficit by radiation is compensated by an effective average energy input of +4.3 $\mathrm{W\,m^2}$ from the turbulent sensible and latent heat fluxes. During the accumulation period more energy is lost by the strong negative radiation budget than gained by turbulent fluxes, which leads to an overall negative surface energy balance (SEB, −3.7 $\mathrm{W\,m^2}$). In July, the SEB is stongly positive with +37.4 $\mathrm{W\,m^2}$ due to the radiation input (+34.3 $\mathrm{W\,m^2}$) and turbulent sensible heat flux (+4.5 $\mathrm{W\,m^2}$). In contrast, during the ablation season the turbulent latent heat flux is slightly negative (−1.44 $\mathrm{W\,m^2}$). In total there is a mean annual surplus of energy of about +2.67 $\mathrm{W\,m^2}$. Karner et al. (2013) demonstrated for another site some 100 m below KNG8 (see Fig. 1, that the 10 year average surplus is about +9.5 W m^2. The pronounced local differences in the SEB components on Kongsvegen emphasizes that the results of this analysis cannot be generalized, which imposes the need considering characteristic zones on the glacier separately.

3.2 Uncertainty estimation

The integrated model uncertainty for snow height is estimated from a set of Monte-Carlo runs, based on the reference run and specified uncertainty measures of key input factors and model parameters (Table 2). The probability density distributions of the measurement errors are either derived from simultaneous measurements with two sensors, as in case of air temperature measurements, or by the accuracy of the sensor given by the manufacturer specifications. Dealing with measurement errors, there is usually no information on how these uncertainties are distributed and it is not always obvious which uncertainties are taken into account by the manufacturers. In addition, other sources of uncertainty such as aging or radiation effects on temperature sensors are usually not known, but can play a crucial role. Except for the roughness length and the pore volume fraction which are assumed to vary uniformly in the pre-defined range, we follow the common approach and assign normally distributed errors with the SD given by the sensor's accuracy. The uniform distribution of the roughness length is justified by the fact, that throughout the uppermost parts of the Kongsvegen the spatial distribution of snow is strongly influenced by snowdrift that results in frequent sastrugi formation (wind induced dunes) and high local-scale and temporal variability of surface roughness (Sauter et al., 2013). It seems also reasonable to use a uniform range of pore volume fractions rather than assuming a truncated normal distribution. From the distributions a low-discrepancy Sobol sequence has been generated with a total number 16 000 ensemble members (Saltelli et al., 2006). These sequences are commonly used in sensitivity analysis and provide better estimates of the model-free sensitivity measures (see Sect. 3.3).

GMDD
8, 2807–2845, 2015
Assessment of the uncertainty of snowpack simulations
T. Sauter and F. Obleitner

Figure 6 shows the time series of snow depth for the reference run as well as of the quantiles estimated from the ensemble simulations. The 95 % quantile range can be clearly divided into two regimes: (i) the build up of the snow pack when the 95 % interquantile range increases towards ±1.2 m until end of June, and (ii) the melt period when the interquantile range experiences an additional increase. At the end of the one-year simulation period the uncertainty (95 % quantile range) in snow depth caused by the systematic measurements errors reach more than 3 m. Note, that the interquantile range shows a clear asymmetry which is more pronounced after June 2011. At this time the snowpack contains higher fraction of liquid water which decreases the albedo and increases the compaction by wet snow metamorphism. Obviously, the system becomes more sensitive once the old firn i.e. snow from the previous year, with higher densities and lower albedo, re-appears at the surface. Sporadic snowfall events (depending on the temperature threshold) in August 2011 also lead to an increase of the upper 99 % quantile bound. The simulation is also very sensitive in the first two months when the amounts of snowfall are small. Then, uncertainties in the input quantities are decisive whether the new snow remains on the ground or disappears.

While the Monte-Carlo runs offer a good and practical way to quantify the model uncertainty regarding snow height simulations, it provides no qualitative information on the contribution of each input factor. We should also keep in mind, that all factors are independently varied at the same time and interactions are likely to be important. This issue is addressed by taking advantage of the ensemble runs and further decompose the ensemble variability by GSA.

3.3 Decomposition of the model uncertainty

To understand the contribution of individual factors to the ensemble variability, the complete sensitivity pattern need to be considered. In the following section, different sources of uncertainty are estimated using the variance-based GSA method introduced in Sect. 2.3. For all factors the first- and total-order indices are calculated. Figure 7 shows the mean contribution of the factors on the variability of calculated snow depth

GMDD
8, 2807–2845, 2015

changes, surface energy balance (SEB), and the turbulent heat fluxes for three month periods which roughly correspond to seasons. Recall that first-order indices S_i measure individual factor contributions to the ensemble variance, while the total-order indices S_{T_i} also include all interaction effects. The results show that first-order impacts on calculated snow height are dominated by uncertainties of precipitation P and incoming longwave radiation LW (high S_i values). The remaining factors are very likely to have little impact. In the period from May to October, the LW explains 50–60 % of the variance, while P explains around 35–45 %. During the accumulation period precipitation becomes the dominant factor and shows first-order indices between 55–70 %. Over the entire simulation period, individual variables account on average for 93 % (sum of first-order indices) of the total ensemble variance, and thus the remaining 7 % is due to interaction effects. In order to make an important contribution to the ensemble spread the total-order indices should exceed the 0.05 limit (Saltelli et al., 2006). Following this criteria some factors (T, Q, and PVOL) can be designated as insensitive with little influence on the simulated snow depth changes. Moreover, there is a clear evidence that uncertainties in LW by far comprise most to the uncertainty in calculating the SEB components (see Fig. 7). Surprisingly shortwave radiation SW only exceeds the 0.05 limit in spring, while in summer values are very low. In this period U and z_0 are the only factors besides the LW with noticeable impact on the model uncertainty.

The mean seasonal indices can be somehow misleading and impacts might be underestimated in some cases. For example, according to Fig. 7 one might conclude that the z_0 has hardly any impact on snow depth changes and even little effect on the SEB. Having a closer look at the temporal evolution of the indices derived for the SEB (see Fig. 8), however, provides some interesting insights. In the summer season sporadic episodes of strong wind events lead to sudden jumps of the first-order indices of z_0 and U, in which these factors explain together up to 50 % of the total model uncertainty.

GMDD
8, 2807–2845, 2015

Assessment of the uncertainty of snowpack simulations

T. Sauter and F. Obleitner

4 Discussion

For the following discussion we like to remind, that measurement uncertainties are independently sampled and do not possess any correlation structures. Consequently, the approach can not be used to investigate the response of snow or ice depending on e.g. changes in the environmental (climate) conditions. There, some factors show strong coherences, such as LW and T. In order to study climate sensitivity, the input factor set needs a more sophisticated sampling strategy to obtain the same correlation structure as those observed in nature.

However, the decomposition of the model uncertainty by GSA turned out to be an efficient way to provide an enhanced understanding of the model's sensitivity pattern in response to input and model parameter uncertainties. The results are very helpful to establish priorities in research to constrain influencing factors which need to be measured more accurately in order to reduce the total model uncertainty. According to the analysis, about 93 % of the ensemble spread can be explained by linear effects (first-order), while the remaining part is due to factor interactions. The results clearly proof, that linear methods such as sigma-normalized derivatives are insufficient to recover the entire variance as they neither account for interactions nor for non-additivity. In some cases this could lead to an underestimation of the factor's importance, and wrong conclusions may be drawn. As shown by this study, first-order indices may be very close to zero, but they still can make an important contribution to the model's variability by interactions. Based on the GSA outcomes, the following conclusions can be drawn for this specific high Arctic site:

Precipitation. Precipitation measurements are usually fraught with large uncertainties either by wind-induced under-catch, or by the conversion of snow depth changes to precipitation rates in terms of SWE (see also Sect. 2.2). According to Eq. (4) the conversion is sensitive to air temperature ($\partial\rho/\partial T_{\mathrm{air}} = b_\rho$) and wind velocity ($\partial\rho/\partial U = c_\rho/(2\cdot\sqrt{U})$). Obviously, the fresh snow density calculations are in particular sensitive to measurement errors at low wind speed. As shown in Sect. 3.3 the input uncertainty

Discussion Paper | Discussion Paper | Discussion Paper | Discussion Paper |

GMDD

8, 2807–2845, 2015

related to precipitation has a strong impact on the calculated snow depths all year. Increasing the accuracy of the measurements would drastically (by 50–70 %) reduce the uncertainty in the accumulation season, and even by 30–50 % in the ablation season. Schmucki et al. (2014) showed, that for standard precipitation measurements a correction of under-catch may reduce the mean absolute percentage error by 14 % for snow depth at high alpine stations. Førland and Hanssen-Bauer (2000) demonstrated the importance of this issue for Svalbard environments, too. Snowfall events are less frequent in summer time due to the temperature dependence (interaction with temperature), and thus lead to a drop of S_i values. However, episodic snowfall events in summer temporarily do have an impact on the SEB, but the overall contribution is low.

Longwave radiation. Weather stations rarely directly measure the longwave radiation, and the flux often needs to be parametrized by measured quantities such as temperature, humidity, shortwave radiation or cloudiness. The uncertainty in longwave incoming radiation determines 80–87 % of the ensemble variance of the SEB and only a minor contribution comes from the remaining factors. The is mainly due to the strong link between LW and the snow surface temperature, which in turn directly affects the calculation of the turbulent fluxes. Between 60–85 % of the uncertainty in sensible heat flux and 40–65 % of the latent heat flux can be attributed to errors in LW (see Fig. 8). Better estimates can be expected using measured snow surface temperature as direct model input, as suggested by Lehning et al. (1999). Depending on the application, such replacement of prognostic variables by observations may be considered as a methodical step backwards. While the SEB is very sensitive to LW throughout the whole year, its impact on snow depth changes shows a pronounced seasonal cycle. This cycle is related to the variations in the LW mean intensity, varying from 255 $\mathrm{W\,m^{-2}}$ in summer to 226 $\mathrm{W\,m^{-2}}$ in winter. This also emphasizes the importance of LW for melting processes which hitherto has been underestimated generally.

Shortwave Radiation. During the arctic winter shortwave radiation is zero, and so are the first-order influences. The only noticeable contribution is observed in the period from May to July with S_i values up to 4 %. Indeed, this makes SW the second most important factor on the SEB in summer, but its impact on SEB is too little to have a significant influence on the calculated snow depth changes. This is not in line with former studies (Karner et al., 2013) and contrasts intuition. The reason for that can be deduced from a simple analysis, whereby the energies supplied by uncertainties in LW and SW measurements are put in relation. The sensitivity of the net shortwave radiation ∂G due to measurement errors ∂E_{SW} is given by $\partial G / \partial E_{SW} = 1 - \alpha$, with α denoting albedo. Obviously, the effect on the net shortwave radiation flux by small errors in the measurement is solely a function of the albedo. The ratio R of the sensitivties of the incoming longwave radiation and the available shortwave radiation at the ground is therefore $R = 1/(1 - \alpha)$. By multiplying R with the error ratio we obtain the properly scaled ratio $\hat{R} = (E_{LW}/E_{SW}) \cdot (1/(1-\alpha))$. Assuming a 10 % error of typical daytime values in summer ($E_{SW} = 40\,\mathrm{W\,m}^2$, and $E_{LW} = 26\,\mathrm{W\,m}^2$) and a $\alpha = 0.75$, we obtain $\hat{R} = 2.6$. This means the energy supplied by measurement uncertainty of LW is about 2.6 times greater than the energy supplied by measurement uncertainty of SW. In spring and autumn the ratio becomes larger due to increasing albedo and decreasing incoming shortwave radiation. This leads to the conclusion, that increasing the accuracy of SW measurements by a few percent would not increase our confidence in simulations of snow depth or the SEB components.

Temperature. Although the turbulent heat flux is parametrized by measured air temperature differences between the observation and the snow surface temperature, small measurements errors (±0.3 K) have almost no impact on the calculated turbulent fluxes, and hence on calculated snow depth changes. In part this may also be related to a negative feedbacks. Thus, higher air temperature induce enhanced energy transport towards the surface, leading to higher surface temperature. The latter is effectively counterbalanced by enhanced emission of longwave radiation. The only amplifying interaction is most likely with precipitation when temperatures are close to the phase transition threshold. Notable however, measurement uncertainties can be much larger using e.g. less effective (i.e. unventilated) radiation shields for the measurement of air temperature which is still common practise (Karner et al., 2013; Smeets, 2006).

GMDD
8, 2807–2845, 2015

Humidity. The turbulent latent heat flux is parametrized by the difference of the atmospheric humidity in the surface layer and the saturation specific humidity above the snow surface, which is a function of the snow surface temperature. The weak seasonal variability of total-order indices (see Fig. 7 upper panel) can be attributed to the interplay between saturation deficit, temperature and wind speed. Particularly in spring, conditions are favourable when high saturation deficits occur simultaneously with strong winds and moderate temperatures (Sauter et al., 2013; Obleitner and Lehning, 2004; Karner et al., 2013). Nevertheless, values are very low and a better accuracy would not reduce much the ensemble spread of the snow depth simulations.

Windspeed and roughness length. As discussed in Sect. 3.3, the mean sensitivity measures are not very meaningful for U and z_0. Both, the mean S_i and S_{T_i}, are rather low, but temporarily the factors turn out to be most dominant as shown in Fig. 8. The accuracy of both factors are decisive for the estimation of the turbulent fluxes. Together, the quantities explain about 20 % of the uncertainty in the sensible heat flux in summer, and more than 35 % in latent heat flux in winter. More accurate measurements of both quantities could reduce the ensemble spread by almost 8–10 % in the period from August to January. The largest sensitivity is associated with low wind velocities. This lines up with the finding from Dadic et al. (2013), who found highest sensitivity of the turbulent fluxes with respect to wind speed in the range of 3–5 $\mathrm{m\,s^{-1}}$. Furthermore, the effect of local wind velocity variations on turbulent fluxes and the net melt calculations have been demonstrated by several other studies (Dadic et al., 2013; Mott et al., 2013; Marks et al., 1998). While the turbulent fluxes are sensitive to uncertainties of both z_0 and U all year, the impact on the SEB almost vanishes in the summer time due to different signs of the turbulent fluxes (see Sect. 3.1).

Maximum liquid water holding capacity. Liquid water holding capacity of snow is difficult to measure and strongly depends on snow microstructure and related surface/subsurface developments throughout the winter season. Fortunately however, our results indicate that the liquid water holding capacity of snow makes only a small contribution to the total model variance, mainly by interactions. In fact, total-order indices are slightly higher in the melting season but the overall impact on SEB and snow depth changes is negligible.

Karner et al. (2013) and Obleitner and Lehning (2004) likewise estimated the effect of measurement uncertainties on the energy and mass balance at KNG6 on the Kongsvegen glacier (see Fig. 1). In contrary to our findings, they identified SW and T to be very influential factors for the SEB. U and z_0, on the other hand, had no significant impact on the model's uncertainty. However, their estimates were based on consideration of plain first order effects and are therefore not directly comparable to the results given here. It is nevertheless important to note that different sensitivity patterns are likely to exist at different elevation zones of individual glaciers. Further investigation of this issue was beyond the scope of this work.

5 Conclusions

As this study shows, conservatively estimated measurement errors can lead to a significant loss of confidence in snowpack simulations. In our example, the 95 % interquantile range of the ensemble members showed a spread of approximately 3 m at the end of the simulation period, solely caused by key input and parametrization errors. For example, accurate observations of snow depth changes or associated water equivalents are in the rarest cases available. In remote areas scientist usually rely on snow depth measurements by ultrasonic sensors. Unfortunately, this kind of observation has some unavoidable disadvantages: firstly, these measurements are affected by blowing snow, intense snowfall, or extreme temperatures; and secondly, snow depth changes need to be converted to snow water equivalent. Besides the inherent errors by the sensor itself, the environmental boundary conditions introduce a considerable amount of noise, which needs to be reduced. Small-scale fluctuations are usually reduced by filtering techniques, or sometimes even by more sophisticated approaches. Nevertheless, the accuracy of automatic observations will always contain a significant amount of uncertainty, and it is remains difficult to make any statement about its reliability. Nevertheless,

GMDD
8, 2807–2845, 2015

the GSA proofed to be a useful tool to decompose the variance of the snow model, and provides clear evidence on the impact of uncertainties from individual factors as well as by their interaction. The present analysis clearly demonstrates that up to 70 % of the model uncertainty could be reduced, in case a better accuracy in precipitation observations is achieved. More confidence in the simulations, however, can be gained more easily by using direct measurements of LW, rather than parametrizing this flux with other measured quantities (which is often necessary but are affected by larger uncertainties). Even if direct measurements are available, up to 60 % of the snow depth uncertainty is caused by LW measurement errors. The impact on calculated snow depth is related to uncertainties in the SEB, which is determined by approximately 82 % by the LW flux. Although the accuracy of the incoming SW measurement is in the same order of magnitude as the LW measurements, its contribution to the uncertainty of the simulation results is considerable less. The lower proportion is related to the year-round high albedo values at this site, and the associated lower net shortwave radiation flux. As follows from the GSA, errors related to wind measurements and roughness length show episodic effects on the SEB (up to 10 %) due to their impact on the turbulent fluxes. Especially in wintertime failure of wind measurements are frequent and data gaps need to be filled in order to perform year round simulations. Together with missing information about the roughness length, the associated error propagation can significantly diminish the confidence in the modelled SEB. Other quantities, such as T and Q are often measured directly with higher accuracy and hence do not affect significantly the model results. It is finally noted again that the relative impact of individual error sources is very likely to vary for different zones on the glacier, and may show a different sensitivity pattern for other climatic regions. Investigation of this issue is one of the obvious applications of GSA in the future. GSA itself proved a promising tool to entangle the sensitivity of snow models and inherent critical parameters. The presented approach is universal and can be applied to earth systems models in general. Limitations from the practical and methodical point of view concern the high computational effort and proper specification of the probability density functions of parameter uncertainties.

GMDD
8, 2807–2845, 2015

T. Sauter and F. Obleitner

Acknowledgements. This work was basically supported by the Austrian Science Fund (FWF, grant I 369-B17). Field work at Kongsvegen was performed in cooperation with the Norwegian Polar Institute (Tromsøe, J. Kohler) and University of Oslo (Ch. Nuuth). The achievement of snow data was supported by Österreichische Polarforschungsgesellschaft, Julius-Payer Stipendium 2010. F. Karner, F. Bilgeri and W. Steinkogler are thanked for performing field work and pre-evaluation of data used within this study.

References

Armstrong, R. L. and Brun, E.: Snow and climate: physical processes, surface energy exchange and modeling, Cambridge University Press, 2008. 2812

Beersma, J. J. and Buishand, T. A.: Multi-site simulation of daily precipitation and temperature conditional on the atmospheric circulation, Clim. Res., 25, 121–133, 2003. 2815

Bellaire, S., Jamieson, J. B., and Fierz, C.: Corrigendum to "Forcing the snow-cover model SNOWPACK with forecasted weather data" published in The Cryosphere, 5, 1115–1125, 2011, The Cryosphere, 7, 511–513, doi:10.5194/tc-7-511-2013, 2013. 2809

Bernhardt, M., Liston, G. E., Strasser, U., Zängl, G., and Schulz, K.: High resolution modelling of snow transport in complex terrain using downscaled MM5 wind fields, The Cryosphere, 4, 99–113, doi:10.5194/tc-4-99-2010, 2010. 2809

Björnsson, H., Gjessing, Y., Hamran, S.-E., Hagen, J. O., Liestøl, O., Pálsson, F., and Erlingsson, B.: The thermal regime of sub-polar glaciers mapped by multi-frequency radio-echo sounding, J. Glaciol., 42, 23–32, 1996. 2819

Braithwaite, R. J. and Zhang, Y.: Sensitivity of mass balance of five Swiss glaciers to temperature changes assessed by tuning a degree-day model, J. Glaciol., 46, 7–14, 2000. 2810

Brandt, O., Kohler, J., and Lüthje, M.: Spatial mapping of multi-year superimposed ice on the glacier Kongsvegen, Svalbard, J. Glaciol., 54, 73–80, 2008. 2813, 2819

Brun, E., David, P., Sudul, M., and Brunot, G.: A numerical model to simulate snow-cover stratigraphy for operational avalanche forecasting, J. Glaciol., 38, 13–22, 1992. 2810, 2811

Brun, E., Vionnet, V., Boone, A., Decharme, B., Peings, Y., Valette, R., Karbou, F., and Morin, S.: Simulation of northern eurasian local snow depth, mass, and density using a detailed snowpack model and meteorological reanalyses, J. Hydrometeorol., 14, 203–219, 2013. 2810

GMDD
8, 2807–2845, 2015
Assessment of the uncertainty of snowpack simulations
T. Sauter and F. Obleitner

Carmagnola, C. M., Morin, S., Lafaysse, M., Domine, F., Lesaffre, B., Lejeune, Y., Picard, G., and Arnaud, L.: Implementation and evaluation of prognostic representations of the optical diameter of snow in the SURFEX/ISBA-Crocus detailed snowpack model, The Cryosphere, 8, 417–437, doi:10.5194/tc-8-417-2014, 2014. 2810

Castebrunet, H., Eckert, N., Giraud, G., Durand, Y., and Morin, S.: Projected changes of snow conditions and avalanche activity in a warming climate: the French Alps over the 2020–2050 and 2070–2100 periods, The Cryosphere, 8, 1673–1697, doi:10.5194/tc-8-1673-2014, 2014. 2810

Dadic, R., Mott, R., Lehning, M., Carenzo, M., Anderson, B., and Mackintosh, A.: Sensitivity of turbulent fluxes to wind speed over snow surfaces in different climatic settings, Adv. Water Resour., 55, 178–189, 2013. 2827

Durand, Y., Giraud, G., Brun, E., Mérindol, L., and Martin, E.: A computer-based system simulating snowpack structures as a tool for regional avalanche forecasting, J. Glaciol., 45, 469–484, 1999. 2809

Durand, Y., Giraud, G., Laternser, M., Etchevers, P., Mérindol, L., and Lesaffre, B.: Reanalysis of 47 years of climate in the French Alps (1958–2005): climatology and trends for snow cover, J. Appl. Meteorol. Clim., 48, 2487–2512, 2009. 2809, 2810

Etchevers, P., Martin, E., Brown, R., Fierz, C., Lejeune, Y., Bazile, E., Boone, A., Dai, Y.-J., Essery, R., Fernandez, A., Gusev, Y., Jordan, R., Koren, V., Kowalczyk, E., Nasonova, N. O., Pyles, R. D., Schlosser, A., Shmakin, A. B., Smirnova, T. G., Strasser, U., Verseghy, D., Ymazaki, T., and Yang, Z.-L.: Validation of the energy budget of an alpine snowpack simulated by several snow models (SnowMIP project), Ann. Glaciol., 38, 150–158, 2004. 2809, 2820

Feng, X., Sahoo, A., Arsenault, K., Houser, P., Luo, Y., and Troy, T. J.: The impact of snow model complexity at three CLPX sites, J. Hydrometeorol., 9, 1464–1481, 2008. 2809

Førland, E. J. and Hanssen-Bauer, I.: Increased precipitation in the Norwegian Arctic: true or false?, Climatic Change, 46, 485–509, 2000. 2825

Franz, K. J., Butcher, P., and Ajami, N. K.: Addressing snow model uncertainty for hydrologic prediction, Adv. Water Resour., 33, 820–832, 2010. 2810

Fréville, H., Brun, E., Picard, G., Tatarinova, N., Arnaud, L., Lanconelli, C., Reijmer, C., and van den Broeke, M.: Using MODIS land surface temperatures and the Crocus snow model to understand the warm bias of ERA-Interim reanalyses at the surface in Antarctica, The Cryosphere, 8, 1361–1373, doi:10.5194/tc-8-1361-2014, 2014. 2810

Fujita, K.: Effect of precipitation seasonality on climatic sensitivity of glacier mass balance, Earth Planet. Sc. Lett., 276, 14–19, 2008. 2810

Gallée, H., Guyomarc'h, G., and Brun, E.: Impact of snow drift on the Antarctic ice sheet surface mass balance: possible sensitivity to snow-surface properties, Bound.-Lay. Meteorol., 99, 1–19, 2001. 2809

Gallet, J.-C., Domine, F., Savarino, J., Dumont, M., and Brun, E.: The growth of sublimation crystals and surface hoar on the Antarctic plateau, The Cryosphere, 8, 1205–1215, doi:10.5194/tc-8-1205-2014, 2014. 2810

Gerbaux, M., Genthon, C., Etchevers, P., Vincent, C., and Dedieu, J.: Surface mass balance of glaciers in the French Alps: distributed modeling and sensitivity to climate change, J. Glaciol., 51, 561–572, 2005. 2810

Greuell, W. and Konzelmann, T.: Numerical modelling of the energy balance and the englacial temperature of the Greenland ice sheet. Calculations for the ETH-Camp location (West Greenland, 1155 m asl), Global Planet. Change, 9, 91–114, 1994. 2810

Greuell, W. and Oerlemans, J.: Sensitivity studies with a mass balance model including temperature profile calculations inside the glacier, Z. Gletscherkd. Glazialgeol., 22, 101–124, 1986. 2810

Gurgiser, W., Mölg, T., Nicholson, L., and Kaser, G.: Mass-balance model parameter transferability on a tropical glacier, J. Glaciol., 59, 845–858, 2013. 2810

He, M., Hogue, T. S., Franz, K. J., Margulis, S. A., and Vrugt, J. A.: Characterizing parameter sensitivity and uncertainty for a snow model across hydroclimatic regimes, Adv. Water Resour., 34, 114–127, 2011. 2810

Karner, F., Obleitner, F., Krismer, T., Kohler, J., and Greuell, W.: A decade of energy and mass balance investigations on the glacier Kongsvegen, Svalbard, J. Geophys. Res.-Atmos., 118, 3986–4000, 2013. 2810, 2813, 2814, 2820, 2826, 2827, 2828

König, M., Wadham, J., Winther, J.-G., Kohler, J., and Nuttall, A.-M.: Detection of superimposed ice on the glaciers Kongsvegen and midre Love'nbreen, Svalbard, using SAR satellite imagery, Ann. Glaciol., 34, 335–342, 2002. 2813

Lehning, M., Bartelt, P., Brown, B., Russi, T., Stöckli, U., and Zimmerli, M.: SNOWPACK model calculations for avalanche warning based upon a new network of weather and snow stations, Cold Reg. Sci. Technol., 30, 145–157, 1999. 2809, 2825

Lehning, M., Völksch, I., Gustafsson, D., Nguyen, T. A., Stähli, M., and Zappa, M.: ALPINE3D: a detailed model of mountain surface processes and its application to snow hydrology, Hydrol. Process., 20, 2111–2128, 2006. 2809

Liston, G. E. and Elder, K.: A distributed snow-evolution modeling system (SnowModel), J. Hydrometeorol., 7, 1259–1276, 2006. 2809

Magnusson, J., Gustafsson, D., Hüsler, F., and Jonas, T.: Assimilation of point SWE data into a distributed snow cover model comparing two contrasting methods, Water Resour. Res., 50, 7816–7835, doi:10.1002/2014WR015302, 2014. 2809

Marks, D., Kimball, J., Tingey, D., and Link, T.: The sensitivity of snowmelt processes to climate conditions and forest cover during rain on snow: a case study of the 1996 Pacific Northwest floow, Hydrol. Process., 12, 1569–1587, 1998. 2827

Mott, R., Gromke, C., Grünewald, T., and Lehning, M.: Relative importance of advective heat transport and boundary layer decoupling in the melt dynamics of a patchy snow cover, Adv. Water Resour., 55, 88–97, 2013. 2827

Obleitner, F. and De Wolde, J.: On intercomparison of instruments used within the Vatnajökull glacio-meteorological experiment, Bound.-Lay. Meteorol., 92, 25–35, 1999. 2820

Obleitner, F. and Lehning, M.: Measurement and simulation of snow and superimposed ice at the Kongsvegen glacier, Svalbard (Spitzbergen), J. Geophys. Res.-Atmos., 109, doi:10.1029/2003JD003945, 2004. 2809, 2813, 2814, 2827, 2828

Oerlemans, J.: Climate sensitivity of glaciers in southern Norway: application of an energy-balance model to Nigardsbreen, Hellstugubreen and Alfotbreen, J. Glaciol., 38, 223–232, 1992. 2810

Phan, X. V., Ferro-Famil, L., Gay, M., Durand, Y., Dumont, M., Morin, S., Allain, S., D'Urso, G., and Girard, A.: 1D-Var multilayer assimilation of X-band SAR data into a detailed snowpack model, The Cryosphere, 8, 1975–1987, doi:10.5194/tc-8-1975-2014, 2014. 2810

Pomeroy, J. and Gray, D.: Saltation of snow, Water Resour. Res., 26, 1583–1594, 1990. 2816

Radić, V. and Hock, R.: Modeling future glacier mass balance and volume changes using ERA-40 reanalysis and climate models: a sensitivity study at Storglaciären, Sweden, J. Geophys. Res.-Earth, 111, F03003, doi:10.1029/2005JF000440, 2006. 2810

Rutter, N., Essery, R., Pomeroy, J., Altimir, N., Andreadis, K., Baker, I., Barr, A., Bartlett, P., Boone, A., Deng, H., Douville, H., Dutra, E., Elder, K., Ellis, C., Feng, Xia, Gelfan, A., Goodbody, A., Gusev, Y., Gustafsson, D., Hellstöm, R., Hirabayashi, Y., Hirota, T., Jonas, T., Koren, V., Kuragina, A., Lettenmaier, D., Li, W.-P., Lice, C., Martin, E., Nasanova, O., Pumpanen, J., Pyles, R. D., Samuelsson, P., Sandells, M., Schädler, G., Shmakin, A., Smirnova, T. G., Stähli, M., Stöckli, R., Strasser, U., Su, H., Suzuki, K., Takata, K., Tanaka, K., Thompson, E., Vesala, T., Viterbo, P., Wiltshire, A., Xia, K., Xue, Y., and Yamazaki, T.: Evaluation of forest snow processes models (SnowMIP2), J. Geophys. Res.-Atmos., 114, D06111, doi:10.1029/2008JD011063, 2009. 2809, 2820

Saltelli, A., Tarantola, S., and Chan, K. P.: A quantitative model-independent method for global sensitivity analysis of model output, Technometrics, 41, 39–56, 1999. 2817

Saltelli, A., Ratto, M., Tarantola, S., and Campolongo, F.: Sensitivity analysis practices: strategies for model-based inference, Reliab. Eng. Syst. Safe., 91, 1109–1125, doi:10.1016/j.ress.2005.11.014, 2006. 2817, 2821, 2823

Saltelli, A., Annoni, P., Azzini, I., Campolongo, F., Ratto, M., and Tarantola, S.: Variance based sensitivity analysis of model output. Design and estimator for the total sensitivity index, Comput. Phys. Commun., 181, 259–270, 2010. 2818

Sauter, T. and Venema, V.: Natural three-dimensional predictor domains for statistical precipitation downscaling, J. Climate, 24, 6132–6145, 2011. 2817

Sauter, T., Möller, M., Finkelnburg, R., Grabiec, M., Scherer, D., and Schneider, C.: Snowdrift modelling for the Vestfonna ice cap, north-eastern Svalbard, The Cryosphere, 7, 1287–1301, doi:10.5194/tc-7-1287-2013, 2013. 2816, 2821, 2827

Schmucki, E., Marty, C., Fierz, C., and Lehning, M.: Evaluation of modelled snow depth and snow water equivalent at three contrasting sites in Switzerland using SNOWPACK simulations driven by different meteorological data input, Cold Reg. Sci. Technol., 99, 27–37, 2014. 2810, 2825

Smeets, C.: Assessing unaspirated temperature measurements using a thermocouple and a physically based model, in: The Mass Budget of Arctic Glaciers, Workshop and GLACIODYN planning meeting, 29 January-3 February 2006, IASC Working group on Arctic Glaciology, Institute for Marine and Amtospheric Research, Utrecht, p. 99, 2006. 2826

Sobol, I. M., Tarantola, S., Gatelli, D., Kucherenko, S., and Mauntz, W.: Estimating the approximation error when fixing unessential factors in global sensitivity analysis, Reliab. Eng. Syst. Safe., 92, 957–960, 2007. 2818

Van de Wal, R. and Oerlemans, J.: An energy balance model for the Greenland ice sheet, Global Planet. Change, 9, 115–131, 1994. 2810

Vionnet, V., Brun, E., Morin, S., Boone, A., Faroux, S., Le Moigne, P., Martin, E., and Willemet, J.-M.: The detailed snowpack scheme Crocus and its implementation in SURFEX v7.2, Geosci. Model Dev., 5, 773–791, doi:10.5194/gmd-5-773-2012, 2012. 2810, 2811, 2814

Wang, T., Ottlé, C., Boone, A., Ciais, P., Brun, E., Morin, S., Krinner, G., Piao, S., and Peng, S.: Evaluation of an improved intermediate complexity snow scheme in the ORCHIDEE land surface model, J. Geophys. Res.-Atmos., 118, 6064–6079, 2013. 2810

Wright, A., Wadham, J., Siegert, M., Luckman, A., Kohler, J., and Nuttall, A.: Modeling the refreezing of meltwater as superimposed ice on a high Arctic glacier: a comparison of approaches, J. Geophys. Res.-Earth, 112, F04016, doi:10.1029/2007JF000818, 2007. 2813

GMDD
8, 2807–2845, 2015

Assessment of the uncertainty of snowpack simulations

T. Sauter and F. Obleitner

Table 1. Model parameters used for the reference run.

Parameter	Value		Description
z_0	0.002	m	Roughness length for momentum
zh_0	0.0002	m	Roughness length for heat
HC_{LW}	0.05	–	Max. liquid water holding capacity
$ALB_{0.3}$	0.38	–	Absorption coefficient for spectral band 0.3–0.8 mm
$ALB_{0.8}$	0.23	–	Absorption coefficient for spectral band 0.8–1.5 mm
$ALB_{1.5}$	0.08	–	Absorption coefficient for spectral band 1.5–2.8 mm
ρ_{thres}	830	$kg\,m^{-3}$	Ice density threshold

GMDD
8, 2807–2845, 2015

Assessment of the uncertainty of snowpack simulations

T. Sauter and F. Obleitner

Table 2. Specification of basic model input uncertainties and assigned probability density functions. The Sobol sequence has been generated from the distributions given in the last column ($\mathcal{N}$ – Normal distribution; $\mathcal{U}$ – Uniform distribution).

Parameter	Description	Uncertainty	Distribution
T_{air}	Air temperature	±0.3 K	$\mathcal{N}(0.00, 0.30)$
RH	Relative humidity	±3.0 %	$\mathcal{N}(0.00, 3.00)$
SW	Shortwave incoming radiation	±10.0 %	$\mathcal{N}(0.00, 0.10)$
LW	Longwave incoming radiation	±10.0 %	$\mathcal{N}(0.00, 0.10)$
U	Wind speed	±0.3 m s^{-1}	$\mathcal{N}(0.00, 0.30)$
P	Precipitation	±25.0 %	$\mathcal{N}(0.00, 0.25)$
z_0	Aerodynamic roughness length	0.001–0.10 m	$\mathcal{U}(0.001, 0.10)$
PVOL	Pore volume fraction for maximum liquid water holding capacity	0.03–0.05%	$\mathcal{U}(0.03, 0.05)$

GMDD
8, 2807–2845, 2015

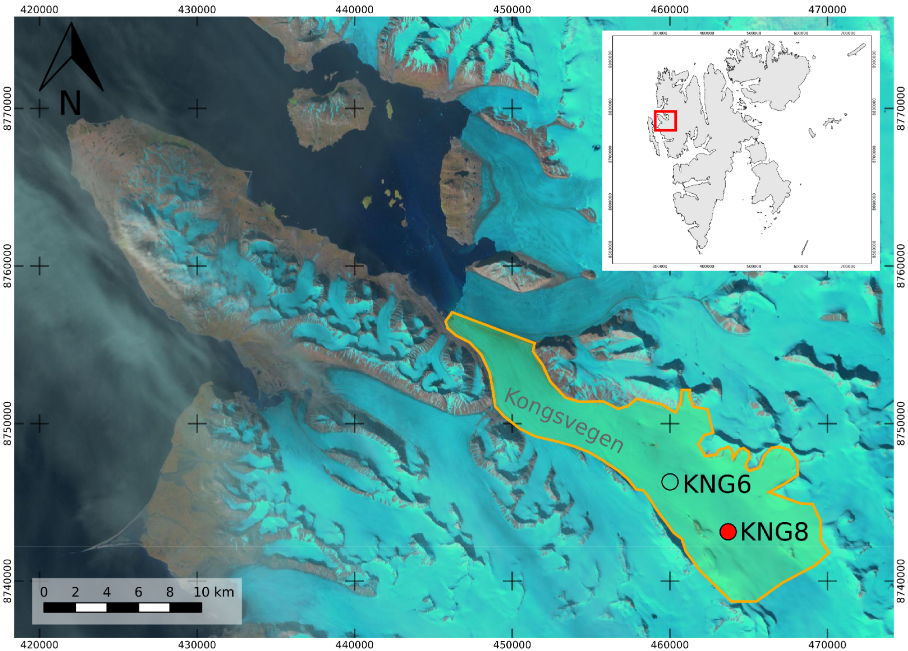

Figure 1. Map demonstrating the location of Kongsvegen glacier within Svalbard and the position of the automatic weather stations KNG8 (red dot) and KNG6 (black circle). The orange outline shows the approximate Kongsvegen extent (optical LandSat 7 image from July 1999, UTM 34N, WGS84).

GMDD
8, 2807–2845, 2015

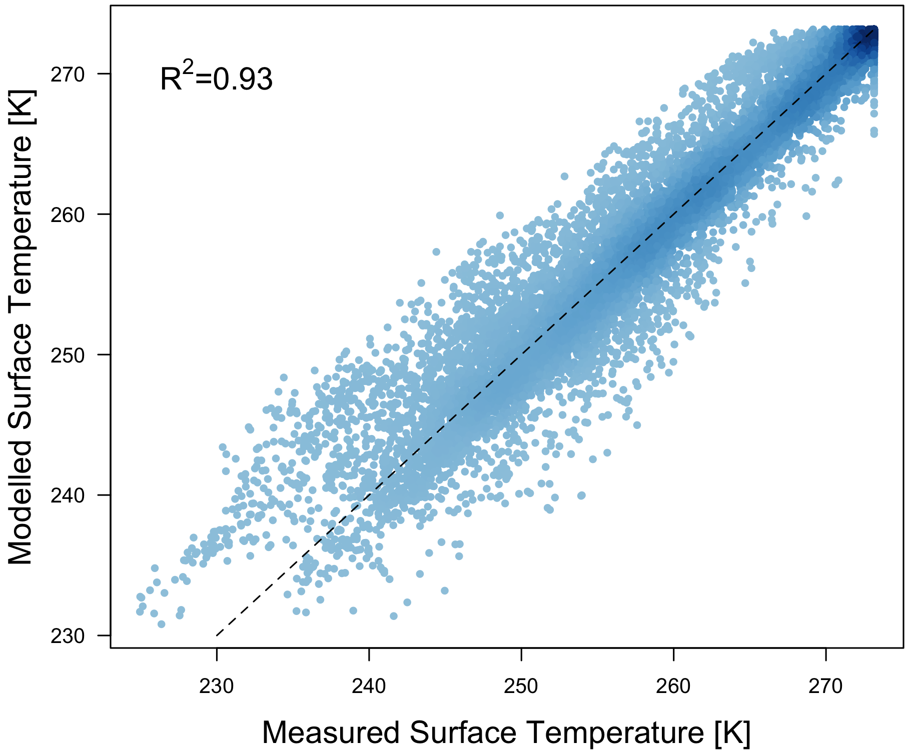

Figure 2. Comparison of the mean 6 hourly modelled and measured snow surface temperatures at the location KNG8.

GMDD
8, 2807–2845, 2015

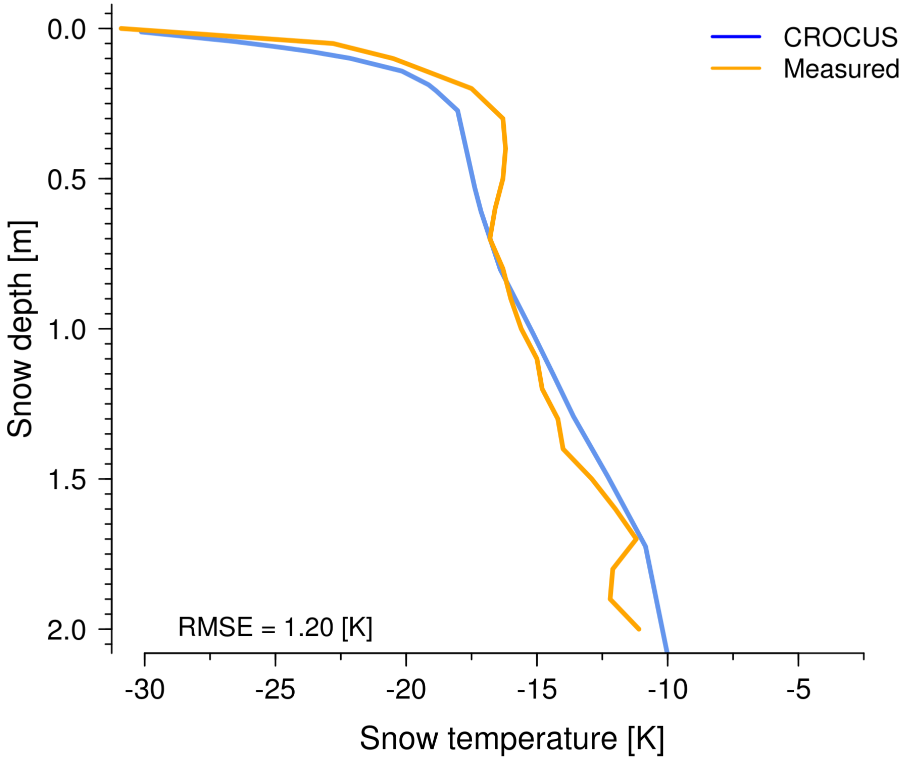

Figure 3. Observed (orange) and modelled (blue) snow temperature profile on 6 April 2011 17:00 UTC at the location KNG8.

GMDD
8, 2807–2845, 2015

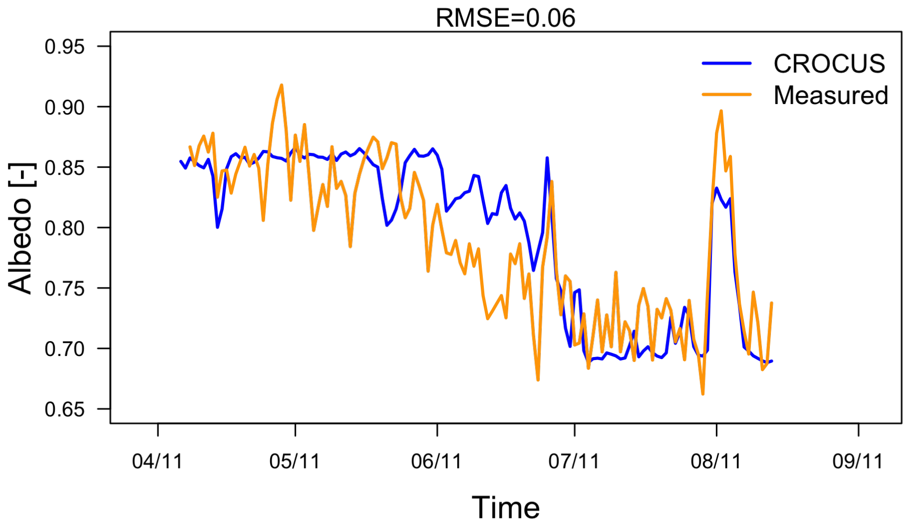

Figure 4. Daily mean observed (orange) and modelled (blue) snow albedo at the location KNG8.

GMDD
8, 2807–2845, 2015

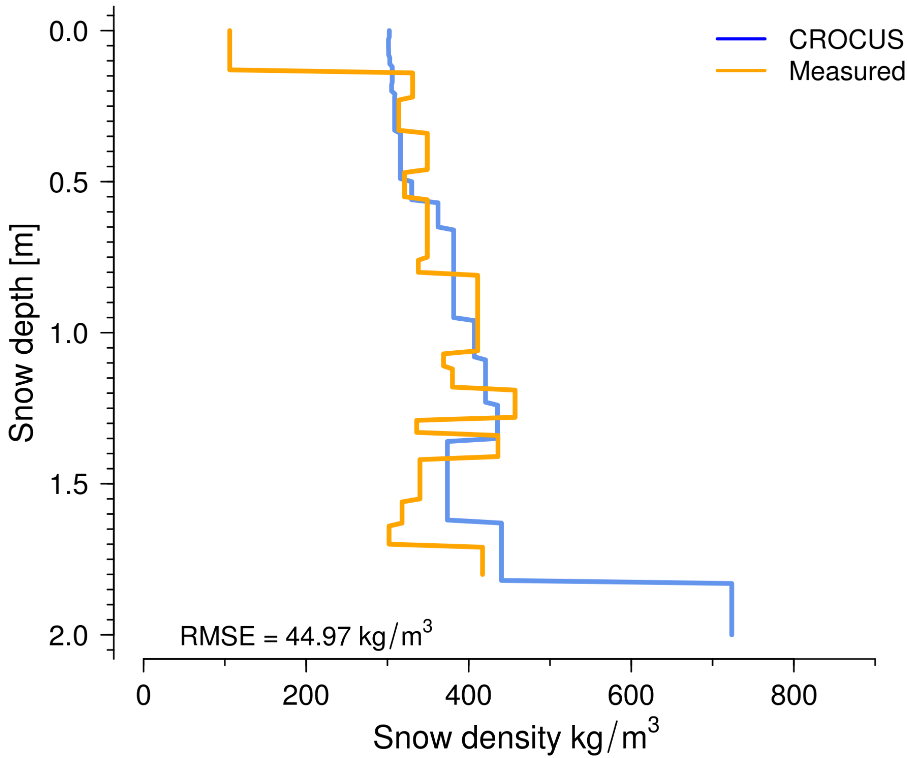

Figure 5. Observed (orange) and modelled (blue) snow density profile on 6 April 2011 at the location KNG8.

GMDD
8, 2807–2845, 2015

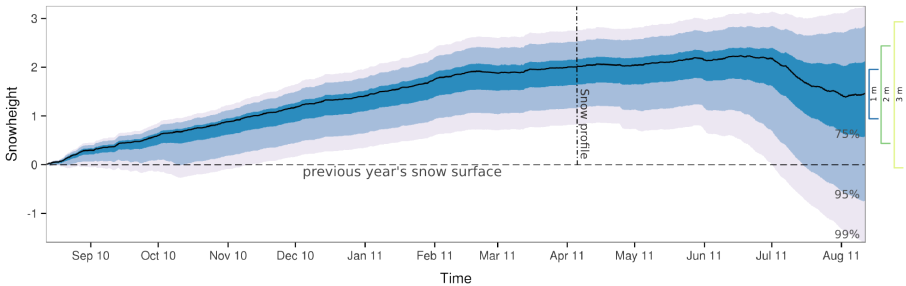

Figure 6. Uncertainty of the model simulation due to propagating uncertainties in the model inputs. The black lines represents the reference run. The intervals show the 99, 95 and 75 % quantiles estimated from the Monte-Carlo runs (16 000 ensemble members).

GMDD
8, 2807–2845, 2015

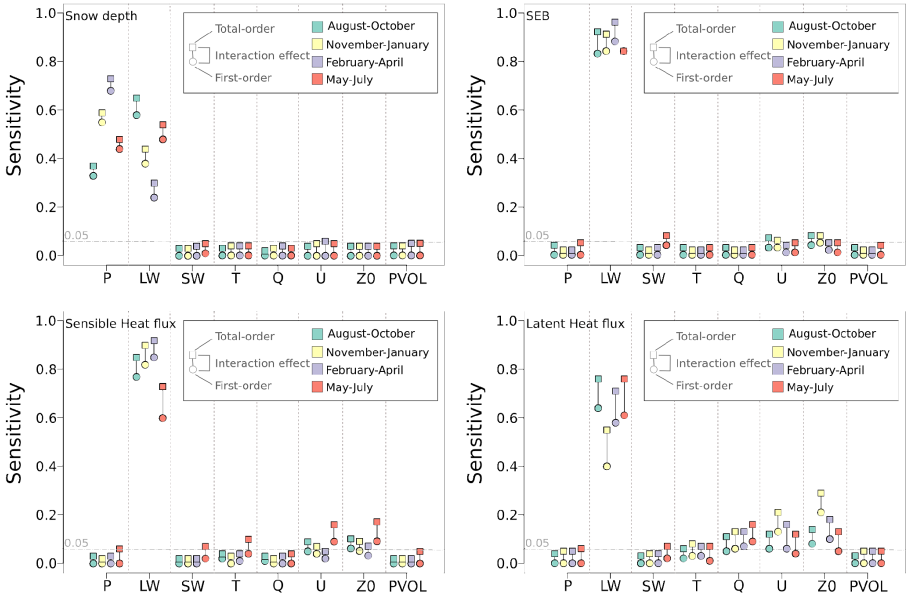

Figure 7. Mean impact of measurement uncertainties for different seasons on snow depth changes, surface energy balance (SEB), sensible heat and latent heat flux.

GMDD
8, 2807–2845, 2015

Assessment of the uncertainty of snowpack simulations

T. Sauter and F. Obleitner

Title Page
Abstract Introduction
Conclusions References
Tables Figures
◀◀ ▶▶
◀ ▶
Back Close
Full Screen / Esc
Printer-friendly Version
Interactive Discussion

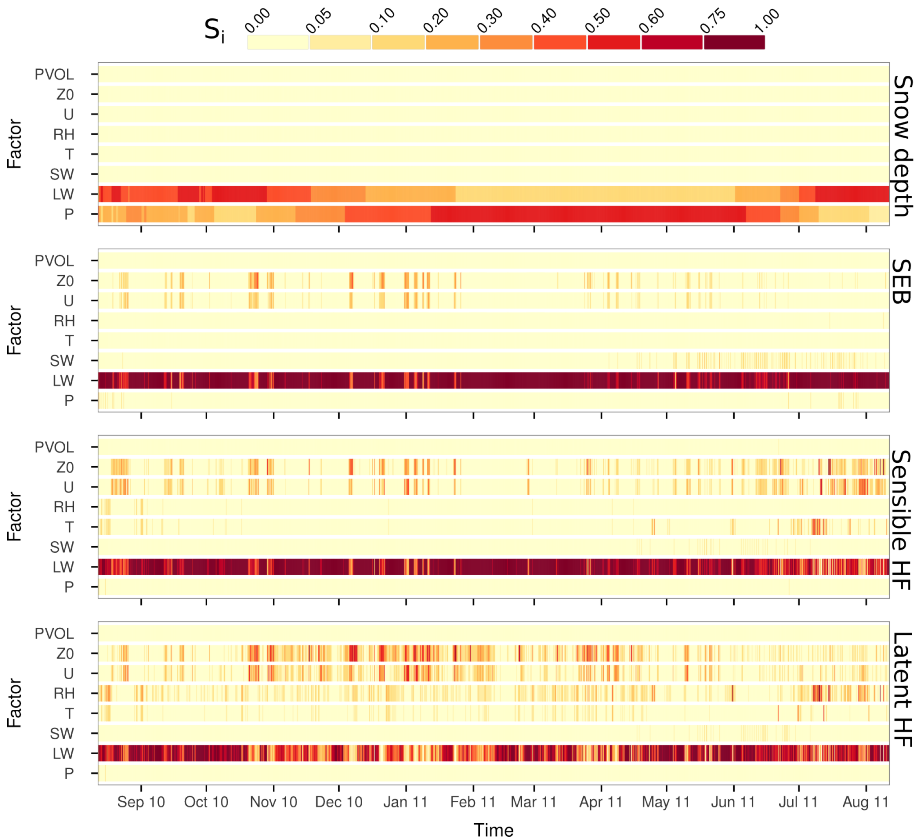

Figure 8. Temporal evolution of the first-order sensitivity indices affecting modelled snow depth changes, surface energy balance (SEB), sensible and latent heat flux at KNG8. Refer to Table 1 for explanation of the indicated uncertainty factors.